

# Heterodivalent Linked Macrocylic $\beta$ -Sheets with Enhanced Activity against $A\beta$ Aggregation: Two Sites Are Better Than One

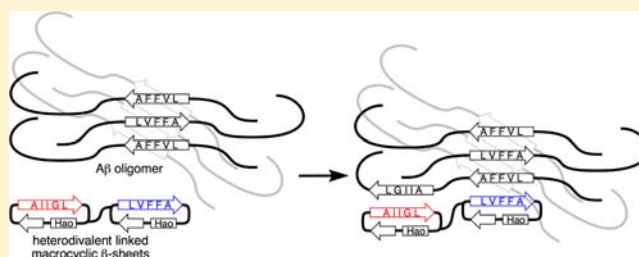
Pin-Nan Cheng,<sup>†</sup> Ryan Spencer,<sup>†</sup> R. Jeremy Woods,<sup>†</sup> Charles G. Glabe,<sup>‡</sup> and James S. Nowick<sup>\*,†</sup>

<sup>†</sup>Department of Chemistry, University of California, Irvine, Irvine, California 92697-2025, United States

<sup>‡</sup>Department of Molecular Biology and Biochemistry, University of California, Irvine, Irvine, California 92697-3900, United States

**S** Supporting Information

**ABSTRACT:** This paper reports a series of heterodivalent linked macrocylic  $\beta$ -sheets **6** that are not only far more active against amyloid- $\beta$  ( $A\beta$ ) aggregation than their monovalent components **1a** and **1b** but also are dramatically more active than their homodivalent counterparts **4** and **5**. The macrocylic  $\beta$ -sheet components **1a** and **1b** comprise pentapeptides derived from the N- and C-terminal regions of  $A\beta$  and molecular template and turn units that enforce a  $\beta$ -sheet structure and block aggregation. Thioflavin T fluorescence assays show that heterodivalent linked macrocylic  $\beta$ -sheets **6** delay  $A\beta_{1-40}$  aggregation 6–8-fold at equimolar concentrations and substantially delay aggregation at substoichiometric concentrations, while homodivalent linked macrocylic  $\beta$ -sheets **4** and **5** and monovalent macrocylic  $\beta$ -sheets **1a** and **1b** only exhibit more modest effects at equimolar or greater concentrations. A model to explain these observations is proposed, in which the inhibitors bind to and stabilize the early  $\beta$ -structured  $A\beta$  oligomers and thus delay aggregation. In this model, heterodivalent linked macrocylic  $\beta$ -sheets **6** bind to the  $\beta$ -structured oligomers more strongly, because N-terminal-derived component **1a** can bind to the N-terminal-based core of the  $\beta$ -structured oligomers, while the C-terminal-derived component **1b** can achieve additional interactions with the C-terminal region of  $A\beta$ . The enhanced activity of the heterodivalent compounds suggests that polyvalent inhibitors that can target multiple regions of amyloidogenic peptides and proteins are better than those that only target a single region.

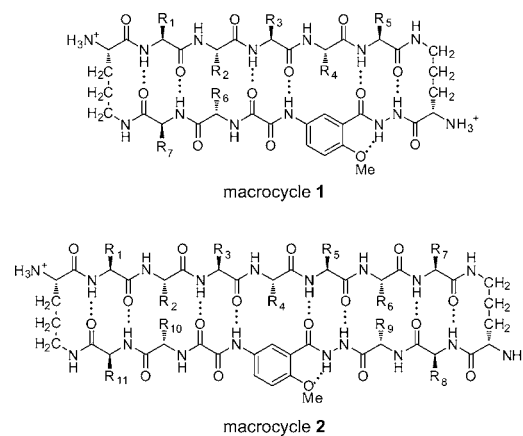


## INTRODUCTION

Amyloid- $\beta$  ( $A\beta$ ) fibrils associated with Alzheimer's disease contain layered  $\beta$ -sheet structures involving  $\beta$ -strands from both the N- and C-terminal regions of  $A\beta$  peptides.<sup>1</sup> NMR-based structural models of  $A\beta$  fibrils show that  $A\beta$  peptides self-assemble into parallel  $\beta$ -sheets that fold into U-shaped superstructures (Figure 1).<sup>2</sup> The two parallel  $\beta$ -sheets of the U-shaped superstructure are layered in an antiparallel fashion. Similar fibril structures also occur in human islet amyloid polypeptide associated with type II diabetes and likely occur more widely in amyloids.<sup>3</sup>

Macrocylic  $\beta$ -sheets containing turn and template units provide useful chemical tools with which to understand and control amyloid aggregation.<sup>4</sup> Our laboratory has introduced 42- and 54-membered ring macrocycles **1** and **2** (Chart 1) that can fold into  $\beta$ -sheet structures and display preorganized  $\beta$ -strands. Macrocycle **1** incorporates a pentapeptide  $\beta$ -strand into the upper strand, while macrocycle **2** incorporates a heptapeptide  $\beta$ -strand. When these macrocycles display amyloidogenic  $\beta$ -strands, they are able to inhibit or suppress amyloid aggregation through  $\beta$ -sheet interactions. We have demonstrated that macrocycles **1** containing pentapeptide VQIVY can inhibit aggregation of the  $\tau$ -derived peptide Ac-VQIVYK-NH<sub>2</sub> (AcPHF6) associated with Alzheimer's disease<sup>5</sup> and that macrocycles **2** containing amyloidogenic heptapeptide

Chart 1



sequences can inhibit aggregation of  $A\beta$ ,  $\beta_2$ -microglobulin and  $\alpha$ -synuclein and can detoxify  $A\beta$  aggregates.<sup>4c,d</sup> We have also demonstrated that the activity of macrocylic  $\beta$ -sheets against  $A\beta$  aggregation can be dramatically enhanced through expansion from macrocycle **1** to **2**.<sup>4d</sup>

Received: June 5, 2012

Published: July 24, 2012

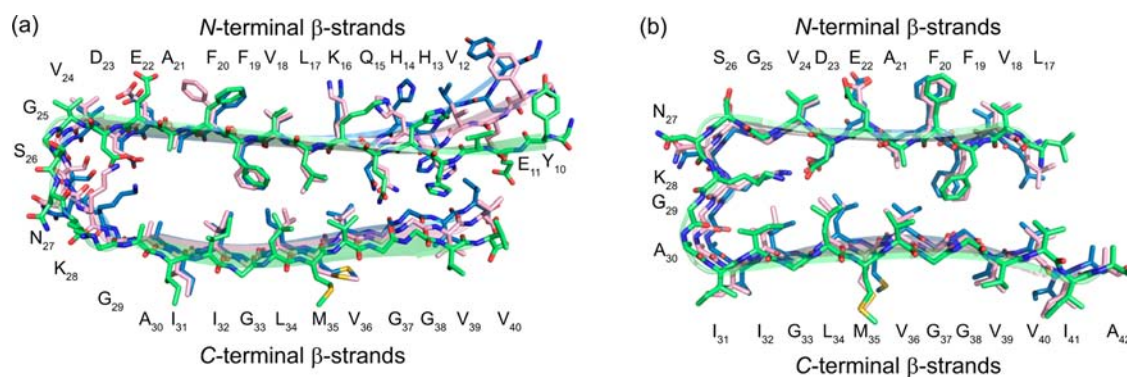
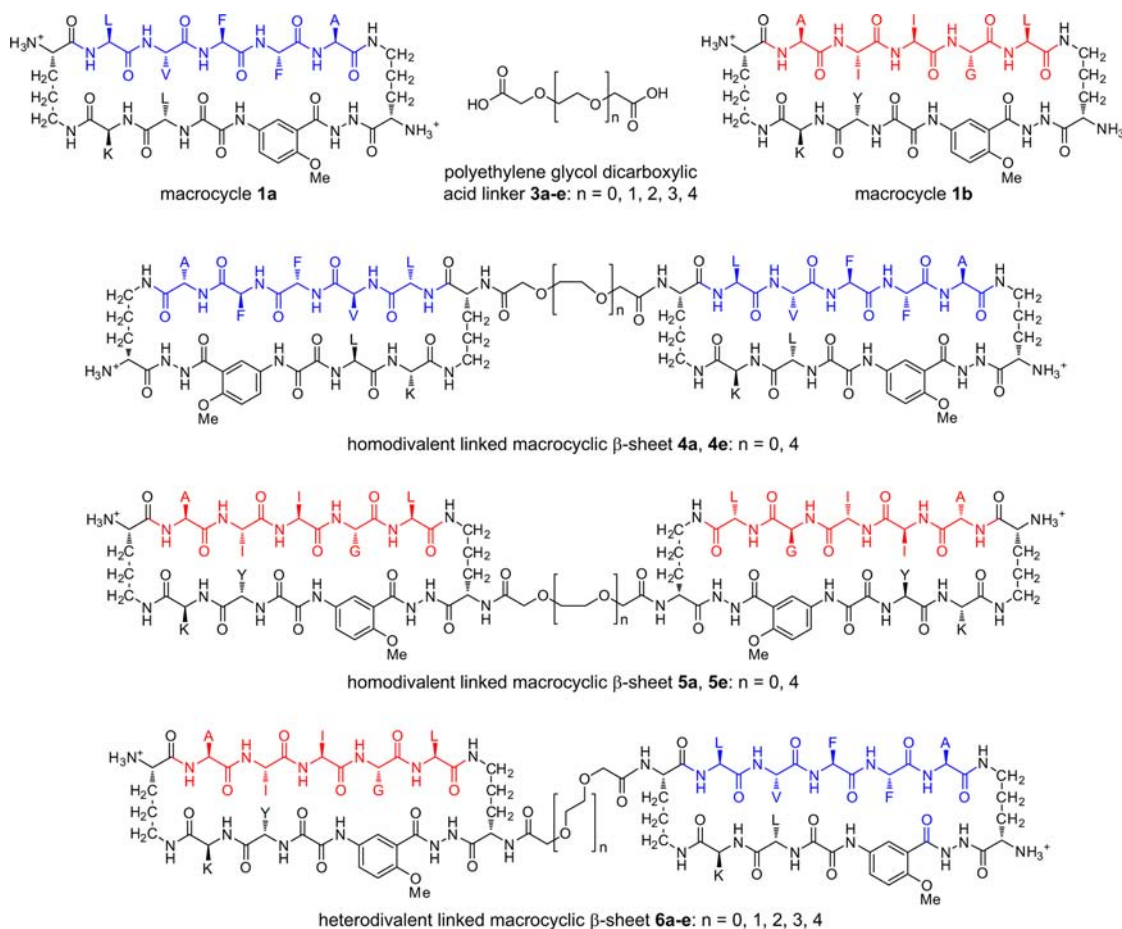


**Figure 1.** NMR-based structural models of  $A\beta$  fibrils. Models of (a)  $A\beta_{1-40}$  and (b)  $A\beta_{1-42}$  fibrils.

## Chart 2

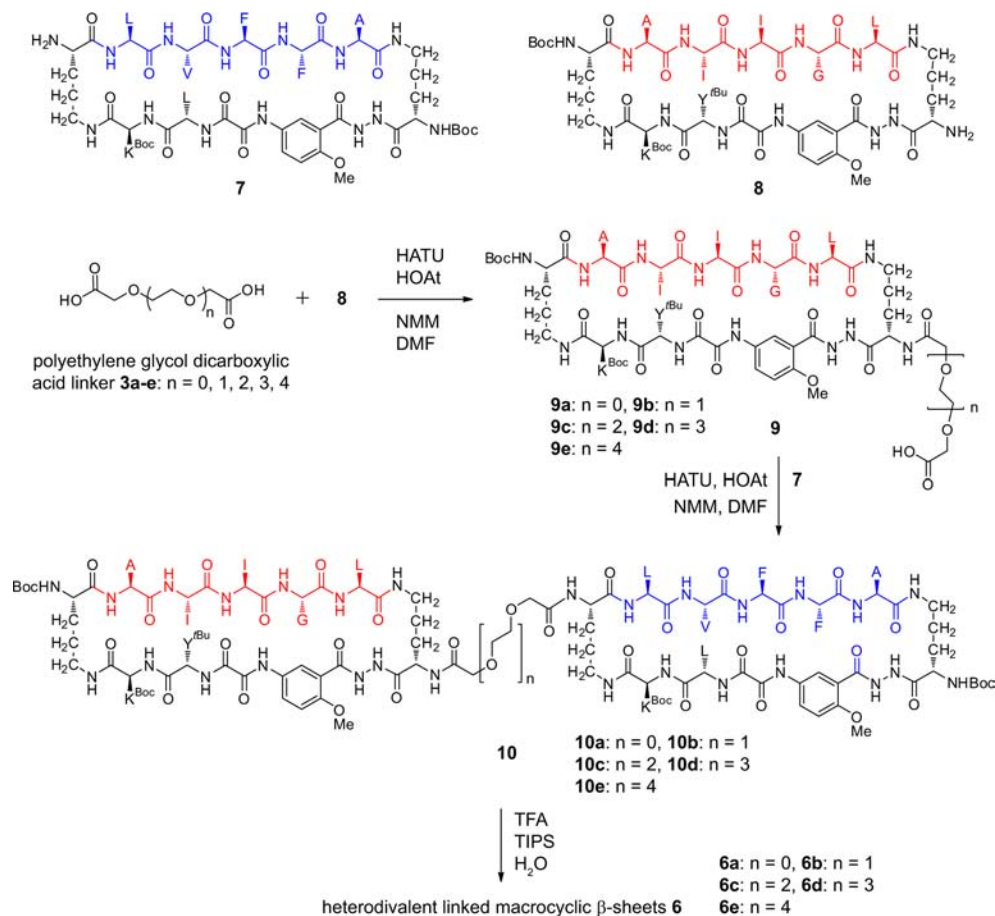


Polyvalency is a powerful means for designing ligands that bind more strongly to targets.<sup>6</sup> We have previously shown that macrocycle **1** can readily be linked to form divalent macrocyclic  $\beta$ -sheet structures that display two  $\beta$ -sheet domains.<sup>4a</sup> Here, we ask whether this divalency can lead to better inhibitors against  $A\beta$  aggregation. To address this question, we designed divalent linked macrocyclic  $\beta$ -sheets by connecting two macrocycles **1** through polyethylene glycol dicarboxylic acid (PEG diacid) linkers **3** (see Chart 2).<sup>7</sup> We also ask whether targeting two different hydrophobic regions of  $A\beta$  with these divalent linked macrocyclic  $\beta$ -sheets would lead to better activity than targeting a single hydrophobic region. To address this question, we designed homodivalent linked macrocyclic  $\beta$ -sheets **4** and **5** and heterodivalent linked macrocyclic  $\beta$ -sheets **6** (Chart 2).

Homodivalent linked macrocyclic  $\beta$ -sheets **4** contain two copies of macrocycle **1a** containing  $A\beta_{17-21}$  ( $R_1-R_5 = LVVFA$ ) linked through PEG diacid linkers, while homodivalent linked macrocyclic  $\beta$ -sheets **5** contain two copies of macrocycle **1b** containing  $A\beta_{30-34}$  ( $R_1-R_5 = AIIGL$ ) linked through PEG diacid linkers. Heterodivalent linked macrocyclic  $\beta$ -sheets **6** contain one copy of macrocycle **1a** and one copy of macrocycle **1b** linked through PEG diacid linkers.

Our studies show that divalent linked macrocyclic  $\beta$ -sheets generally exhibit enhanced activity against  $A\beta$  aggregation and that heterodivalent linked macrocyclic  $\beta$ -sheets **6** are unexpectedly more active than homodivalent linked macrocyclic  $\beta$ -sheets **4** and **5**.

Scheme 1



## RESULTS

### Syntheses of Divalent Linked Macrocyclic $\beta$ -Sheets 4–6

**6.** Divalent  $\beta$ -sheets 4–6 were synthesized by coupling PEG diacid linkers **3** with macrocycles **7** and **8**, which each contain a single free amino group in one of the  $\delta$ -linked ornithine turn units (Scheme 1). Homodivalent  $\beta$ -sheets **4** and **5** were synthesized by coupling macrocycles **7** or **8** with 0.45 mol equiv of the appropriate PEG diacid linkers **3** (Scheme S1). Heterodivalent  $\beta$ -sheets **6a–e** were synthesized by first coupling macrocycle **8** with a 10-fold excess of PEG diacid linkers **3a–e** to give monoacids **9a–e** and then coupling the monoacids with macrocycle **7** (Scheme 1).

**Inhibition of  $A\beta$  Aggregation by Divalent Linked Macrocyclic  $\beta$ -Sheets.** We used thioflavin T (ThT) fluorescence assays to investigate the effects of divalent  $\beta$ -sheets 4–6 and monovalent homologues **1a** and **1b** on  $A\beta_{1-40}$  aggregation.<sup>8</sup> The time course of  $A\beta$  aggregation generally demonstrates a sigmoidal curve, containing a lag phase, a growth phase, and an equilibrium phase (Figure 2a). The duration of the lag phase is widely used as a diagnostic indicator of inhibition of  $A\beta$  aggregation. We thus used this lag time to evaluate the activity of **1a**, **1b**, and 4–6 against  $A\beta_{1-40}$  aggregation.

ThT fluorescence assays show that macrocycle **1a** containing sequence  $A\beta_{17-21}$  slightly delays  $A\beta_{1-40}$  aggregation, macrocycle **1b** containing sequence  $A\beta_{30-34}$  accelerates  $A\beta_{1-40}$  aggregation, and a mixture of 1 mol equiv of macrocycle **1a** and 1 mol equiv of macrocycle **1b** does not significantly change the lag time (Figure 2b). Macrocycle **1a** delays  $A\beta_{1-40}$  aggregation by 30%

at 2 equiv, increasing the lag time from 107 to 143 min, while macrocycle **1b** accelerates  $A\beta_{1-40}$  aggregation by 50%, reducing the lag time from 107 to 57 min. A mixture of 1 equiv of macrocycle **1a** and 1 equiv of macrocycle **1b** exhibits a lag time of 106 min, which is within statistical variation of that of  $A\beta_{1-40}$  alone. These results are consistent with trends that we have observed in the effects of macrocycles **2** against  $A\beta$  aggregation and also support that the central hydrophobic sequence  $A\beta_{17-21}$  plays an important role in  $A\beta$  aggregation and in the activity of macrocycles **1** and **2** against  $A\beta_{1-40}$  aggregation.<sup>4d,9</sup>

ThT fluorescence assays show that heterodivalent  $\beta$ -sheets are not only far more active than their monovalent components but also are dramatically more active against  $A\beta_{1-40}$  aggregation than their homodivalent counterparts. Heterodivalent  $\beta$ -sheets **6a** and **6e** dramatically delay  $A\beta_{1-40}$  aggregation by 570% and 660% respectively at 1 equiv (15  $\mu$ M), while homodivalent  $\beta$ -sheets **4a**, **4e**, and **5e** slightly delay aggregation by 30–70%, and homodivalent  $\beta$ -sheet **5a** accelerates aggregation by 40% (Figure 2c–e). Transmission electron microscopy (TEM) studies of samples taken from the ThT assays indicate that  $A\beta_{1-40}$  forms fibrils in the absence of heterodivalent  $\beta$ -sheet **6e** and does not form fibrils in the presence of heterodivalent  $\beta$ -sheet **6e** during the delayed lag time (Figure 2f).

It is interesting that there is no significant difference in lag time between heterodivalent  $\beta$ -sheet **6a**, which has a short linker ( $n = 0$ ), and heterodivalent  $\beta$ -sheet **6e**, which has a longer linker ( $n = 4$ ). To investigate the effect of the linker length, we synthesized additional heterodivalent  $\beta$ -sheets **6b–d**, which have linkers of intermediate length ( $n = 1–3$ ). ThT

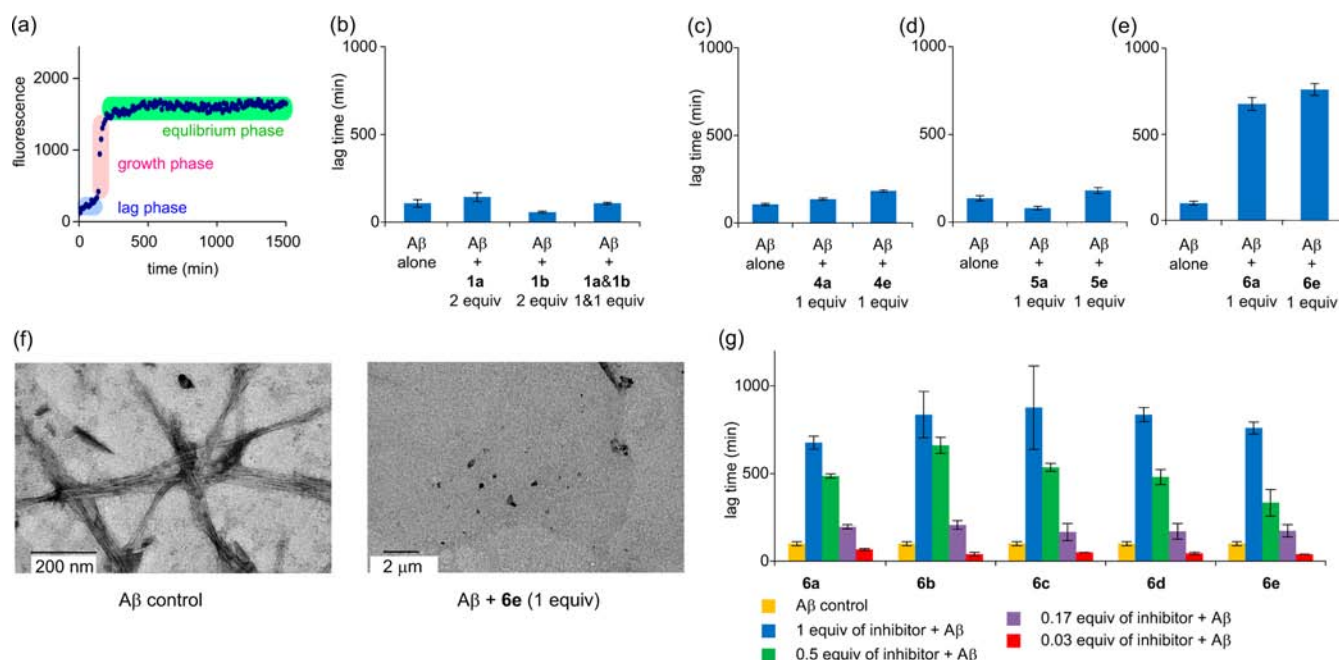


**Figure 2.** ThT fluorescence assays. (a) Fibrillation kinetics of  $A\beta_{1-40}$  monitored by a ThT fluorescence assay. This plot displays three phases of  $A\beta_{1-40}$  aggregation: the lag phase, the growth phase, and the equilibrium phase. (b) Lag time of  $A\beta_{1-40}$  aggregation with and without macrocycles **1a** and **1b**. (c) Lag time of  $A\beta_{1-40}$  aggregation with and without homodivalent  $\beta$ -sheets **4a** and **4e**. (d) Lag time of  $A\beta_{1-40}$  aggregation with and without homodivalent  $\beta$ -sheets **5a** and **5e**. (e) Lag time of  $A\beta_{1-40}$  aggregation with and without heterodivalent  $\beta$ -sheets **6a** and **6e**. (f) TEM image of  $A\beta_{1-40}$  ( $15 \mu\text{M}$ ) after incubation for 6.5 h without (left) and with (right) heterodivalent  $\beta$ -sheet **6e** (1 equiv). (g) Lag time of  $A\beta_{1-40}$  aggregation with heterodivalent  $\beta$ -sheets **6a–e** at 0.03, 0.17, 0.5, and 1 mol equiv. All ThT assays were carried out on  $15 \mu\text{M}$   $A\beta_{1-40}$  in HEPES buffer at  $31^\circ\text{C}$ .

fluorescence assays show that heterodivalent  $\beta$ -sheets **6a–e** delay  $A\beta_{1-40}$  aggregation by 570–770% at 1 equiv (Figure 2g). These results indicate that the size of the PEG-based diacid linkers does not substantially affect the activity of heterodivalent  $\beta$ -sheets **6**. ThT fluorescence assays also show that heterodivalent  $\beta$ -sheets **6** inhibit  $A\beta_{1-40}$  aggregation at substoichiometric concentrations in a dose-dependent manner. Heterodivalent  $\beta$ -sheets **6a–e** delay  $A\beta_{1-40}$  aggregation at 0.17–1.0 equiv ( $2.5$ – $15 \mu\text{M}$ ) by 70–770% (Figure 2g). Surprisingly, heterodivalent  $\beta$ -sheets **6a–e** all nucleate  $A\beta_{1-40}$  aggregation at 0.03 equiv ( $0.5 \mu\text{M}$ ), accelerating  $A\beta_{1-40}$  aggregation by 30–60%. These results indicate that both the activity and the role of the heterodivalent  $\beta$ -sheets in  $A\beta_{1-40}$  aggregation depend on their concentrations.<sup>10</sup>

## DISCUSSION

It is surprising that the heterodivalent linked  $\beta$ -sheets show enhanced inhibitory activity, given that only one of their components inhibits  $A\beta_{1-40}$  aggregation and the other accelerates aggregation. A model based on both nucleation-dependent polymerization and that which we have previously proposed may explain this enhanced inhibition.<sup>4d,11</sup> In this model,  $A\beta_{1-40}$  aggregates to form early  $\beta$ -structured oligomers, which proceed to form a  $\beta$ -structured nucleus, and finally polymerize to form cross- $\beta$  fibrils. Inhibitors bind to and stabilize the early  $\beta$ -structured oligomers and thus delay aggregation, while accelerators create a new, lower energy pathway for aggregation. Figure 3 provides a reaction free-energy diagram for the native, inhibited, and accelerated  $A\beta_{1-40}$  aggregation with black, blue, and red curves. Better inhibitors bind to the early  $\beta$ -structured oligomers more strongly and thus better delay the formation of the  $\beta$ -structured nucleus.<sup>12</sup>

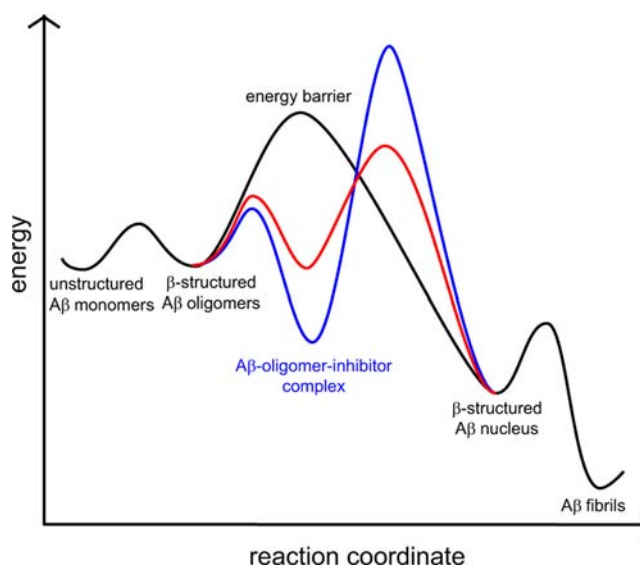


**Figure 3.** Effect of inhibitors and accelerators on the energetics of  $A\beta$  aggregation. The black curve corresponds to a pathway in which  $A\beta_{1-40}$  aggregates without inhibitors, while the blue and red curves correspond to pathways in which  $A\beta_{1-40}$  aggregates with inhibitors and accelerators, respectively.

The hydrophobic N-terminal  $A\beta_{17-21}$  (LVFFA) region forms the core of the  $\beta$ -structured oligomers, in which hydrogen bonding and hydrophobic interactions create a multilayered  $\beta$ -sheet structure (Figure 4a). Similar multilayered  $\beta$ -sheet structures are also observed in macrocycle **1a** and the amyloid-like fibrils formed by peptide fragment  $A\beta_{16-21}$  (KLVFFA).<sup>4b,13</sup> Macrocycle **1a** containing the N-terminal LVFFA pentapeptide complements and binds to the oligomers

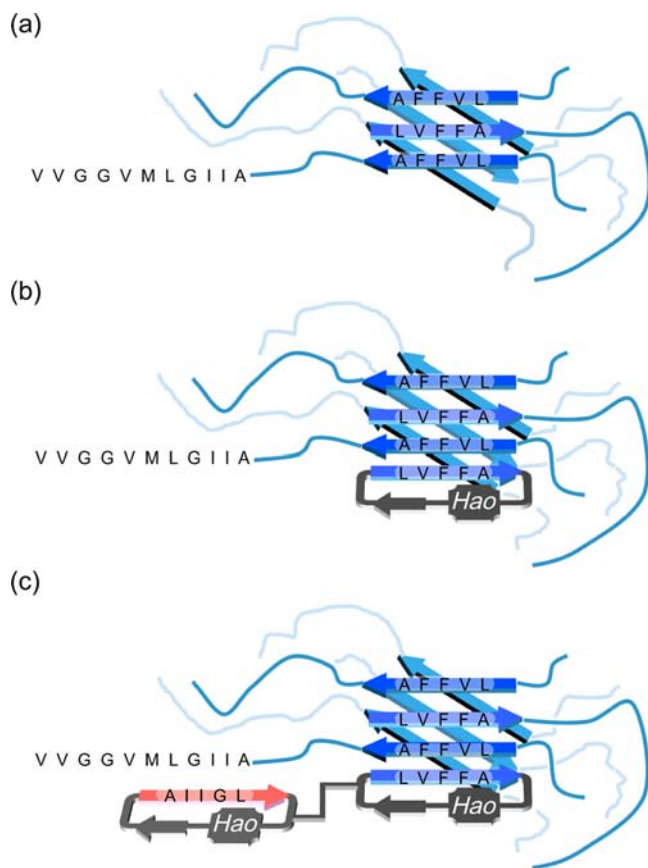


**Figure 4.** Model for enhanced activity of heterodivalent  $\beta$ -sheets **6** against  $A\beta_{1-40}$  aggregation. (a)  $A\beta$  oligomer. (b)  $A\beta$  oligomer-**1a** complex. (c)  $A\beta$  oligomer-**6** complex.

through similar types of interactions and thus inhibits aggregation (Figure 4b). Macrocyclic **1b** containing the C-terminal AIIGL pentapeptide better complements the C-terminal region of  $A\beta_{1-40}$  and facilitates the transition of  $A\beta_{1-40}$  to the U-shaped superstructure associated with fibrils. In the U-shaped superstructure, the C-terminal region also forms  $\beta$ -sheet structure and is packed against the N-terminal region. By facilitating the formation of the U-shaped superstructure, macrocyclic **1b** accelerates aggregation.

The modest effect of homodivalent linkage in **4** and **5** suggests that the  $\beta$ -structured oligomers do not present multiple exposed  $\beta$ -sheet edges in sufficient proximity to be bridged by short PEG linkers. Heterodivalent linked macrocyclic  $\beta$ -sheets **6** bind to the  $\beta$ -structured oligomers more strongly, because the LFFVA-containing macrocycle can bind to the core of the  $\beta$ -structured oligomers, while the AIIGL-containing macrocycle can achieve additional interactions with the C-terminal region of  $A\beta_{1-40}$  (Figure 4c). This working model may provide a framework for the design of even more effective inhibitors that target both the N- and C-terminal regions of  $A\beta$ .

## CONCLUSION

The heterodivalent design of linked macrocyclic  $\beta$ -sheets **6** enhances their activity against  $A\beta$  aggregation. The enhanced activity suggests that polyvalent inhibitors that can target multiple regions of  $A\beta$  are better than ones that only target a single region. The strategy described herein may be applicable

to design inhibitors against aggregation of other amyloid proteins.

## ASSOCIATED CONTENT

### Supporting Information

Details of synthesis of divalent linked macrocyclic  $\beta$ -sheets **4–6**; thioflavin T fluorescence assays of  $A\beta_{1-40}$  with **1a**, **1b**, and **4–6**; TEM; ESIMS and HPLC data of **4–6** and **9**. This material is available free of charge via the Internet at <http://pubs.acs.org>.

## AUTHOR INFORMATION

### Corresponding Author

jsnowick@uci.edu

### Notes

The authors declare no competing financial interest.

## ACKNOWLEDGMENTS

We thank the National Institutes of Health (1R01GM097562 and R01AG033069) for grant support, Dr. Mihaela Necula for helpful guidance and assistance in preliminary experiments, Mr. Ming-Je Sung for assistance in TEM experiments, and Dr. Robert Tycko for providing the coordinates for  $A\beta_{1-40}$  used in Figure 1. We thank Dr. Cong Liu and Dr. David Eisenberg for helpful discussion and insights into the inhibition process.

## REFERENCES

- (1) (a) Roychoudhuri, R.; Yang, M.; Hoshi, M. M.; Teplow, D. B. *J. Biol. Chem.* **2009**, *284*, 4749–4753. (b) Jakob-Roetne, R.; Jacobsen, H. *Angew. Chem., Int. Ed.* **2009**, *48*, 3030–3059.
- (2) (a) Lührs, T.; Ritter, C.; Adrian, M.; Riek-Loher, D.; Bohrmann, B.; Döbeli, H.; Schubert, D.; Riek, R. *Proc. Natl. Acad. Sci. U.S.A.* **2005**, *102*, 17342–17347. (b) Petkova, A. T.; Yau, W.-M.; Tycko, R. *Biochemistry* **2006**, *45*, 498–512.
- (3) (a) Luca, S.; Yau, W.-M.; Leapman, R.; Tycko, R. *Biochemistry* **2007**, *46*, 13505–13522. (b) Hebda, J. A.; Miranker, A. D. *Annu. Rev. Biophys.* **2009**, *38*, 125–152. (c) Wiltzius, J. J. W.; Sievers, S. A.; Sawaya, M. R.; Eisenberg, D. *Protein Sci.* **2009**, *18*, 1521–1530. (d) Middleton, C. T.; Marek, P.; Cao, P.; Chiu, C.-C.; Singh, S.; Woys, A. M.; de Pablo, J. J.; Raleigh, D. P.; Zanni, M. T. *Nat. Chem.* **2012**, *4*, 355–360.
- (4) (a) Woods, R. J.; Brower, J. O.; Castellanos, E.; Hashemzadeh, M.; Khakshoor, O.; Russu, W. A.; Nowick, J. S. *J. Am. Chem. Soc.* **2007**, *129*, 2548–2558. (b) Liu, C.; Sawaya, M. R.; Cheng, P.-N.; Zheng, J.; Nowick, J. S.; Eisenberg, D. *J. Am. Chem. Soc.* **2011**, *133*, 6736–6744. (c) Zheng, J.; Liu, C.; Sawaya, M. R.; Vadla, B.; Khan, S.; Woods, R. J.; Eisenberg, D.; Goux, W. J.; Nowick, J. S. *J. Am. Chem. Soc.* **2011**, *133*, 3144–3157. (d) Cheng, P.-N.; Liu, C.; Zhao, M.; Eisenberg, D.; Nowick, J. S. *Nat. Chem.* **2012**, in press.
- (5) (a) von Bergen, M.; Friedhoff, P.; Biernat, J.; Heberle, J.; Mandelkow, E. M.; Mandelkow, E. *Proc. Natl. Acad. Sci. U.S.A.* **2000**, *97*, 5129–5134. (b) Inouye, H.; Sharma, D.; Goux, W. J.; Kirschner, D. A. *Biophys. J.* **2006**, *90*, 1774–1789.
- (6) (a) Mammen, M.; Choi, S.-K.; Whitesides, G. M. *Angew. Chem., Int. Ed.* **1998**, *37*, 2754–2794. (b) Kim, Y.-S.; Lee, J.-H.; Ryu, J.; Kim, D.-J. *Curr. Pharm. Des.* **2009**, *15*, 637–658.
- (7) (a) Zutshi, R.; Shultz, M. D.; Ulysse, L.; Lutgring, R.; Bishop, P.; Schweitzer, B.; Vogel, K.; Franciskovich, J.; Wilson, M.; Chmielewski, J. *Synlett* **1998**, 1040–1044. (b) Wittmann, V.; Takayama, S.; Gong, K. W.; Weitz-Schmidt, G.; Wong, C.-H. *J. Org. Chem.* **1998**, *63*, 5137–5143.
- (8) LeVine, H. *Methods Enzymol.* **1999**, *309*, 274–284.
- (9) (a) Tjernberg, L. O.; Näslund, J.; Lindqvist, F.; Johansson, J.; Karlström, A. R.; Thyberg, J.; Terenius, L.; Nordstedt, C. *J. Biol. Chem.* **1996**, *271*, 8545–8548. (b) Sciarretta, K. L.; Gordon, D. J.; Meredith, S. C. *Methods Enzymol.* **2006**, *413*, 273–312. (c) Williams, A. D.;

Shivaprasad, S.; Wetzel, R. *J. Mol. Biol.* **2006**, *357*, 1283–1294.

(d) Estrada, L. D.; Soto, C. *Curr. Top. Med. Chem.* **2007**, *7*, 115–126.

(e) Miller, Y.; Ma, B.; Nussinov, R. *Chem. Rev.* **2010**, *110*, 4820–4838.

(10) The acceleration of  $A\beta_{1-40}$  aggregation at low concentrations of heterodivalent  $\beta$ -sheets **6a–e** suggests that **6a–e** may accelerate aggregation in monomeric form and inhibit aggregation in oligomeric form.

(11) Finder, V. H.; Glockshuber, R. *Neurodegener. Dis.* **2007**, *4*, 13–27.

(12) An alternative model for the inhibition involves binding of the heterodivalent inhibitors to the N- and C-terminal  $\beta$ -sheet regions of small  $A\beta$  fibrils and thus the prevention of their elongation by a capping mechanism. The observation that even inhibitors with very short linkers (e.g., **6a**,  $n = 0$ ) block aggregation does not appear to be consistent with this alternative model, because the separation of the N- and C-terminal  $\beta$ -sheet regions of the  $A\beta$  fibrils is larger than the linker (ref 2b).

(13) Colletier, J.-P.; Laganowsky, A.; Landau, M.; Zhao, M.; Soriaga, A. B.; Goldschmidt, L.; Flot, D.; Cascio, D.; Sawaya, M. R.; Eisenberg, D. *Proc. Natl. Acad. Sci. U.S.A.* **2011**, *108*, 16938–16943.